Nonlinear Dyn (2016) 83:1875–1884
DOI 10.1007/s11071-015-2452-z

ORIGINAL PAPER

Nonlinear vibration of the bevel gear with teeth profile modification

Habibollah Motahar · Farhad S. Samani · Moslem Molaie

Received: 18 January 2015 / Accepted: 11 October 2015 / Published online: 20 October 2015

Abstract The prediction of gear vibration and noise has always been a major concern in gear design. Noise and vibration are inevitable problems that are involved in transmission systems; they have intensified when some nonlinear phenomena such as jump phenomenon, tooth separation and period-doubling bifurcation appear in the system. Tip and/or root modifications are well-known solutions that improve dynamic performance of gears. The present work investigates the complex, nonlinear dynamic behavior of three bevel gear models: (1) model with pure involute profile, (2) model with statically optimized tooth profile, and (3) model with dynamically optimized tooth profile. Tooth profile modification is employed in models by means of genetic algorithm in order to extract the best amount and length of modifications. The dynamic responses obtained from dynamic analyzer were compared qualitatively and quantitatively. By augmenting tooth profile modification, the average value of the dynamic responses is decreased intensely for both statically and dynamically optimized gear pairs. Dynamic load factor is calculated and compared with the involute tooth profile model and the two optimized gear sets. Employing teeth optimization leads to elimination of period-2T_m in both optimized simulations.

Keywords Bevel gear vibration · Bifurcation diagram · Tooth profile modification · Dynamic transmission error · Dynamic load factor

H. Motahar · F. S. Samani (✉) · M. Molaie
Department of Mechanical Engineering, Shahid Bahonar University of Kerman, Kerman 76175-133, Iran
e-mail: farhad.samani@uk.ac.ir

H. Motahar
e-mail: Habibollahmotahar@yahoo.com

M. Molaie
e-mail: moslem_molaie@yahoo.com

1 Introduction

Bevel gears are important machine elements, which are used extensively for transmitting power between non-parallel shafts. One of the most common bevel gears is straight bevel gear, which can transmit heavy loads. Dynamic analysis of this type of gear is a controversial issue due to pressing need for achieving higher speed and tolerating heavier load in some applications. Most research carried out to date has focused on spur gear that interestingly expands our understanding of the vibration of gear system.

Transmission error (TE) is the major source of noise and vibration [1]. The common definition of TE is the difference between the actual position of the driven gear and the position it would occupy if the gear drive were perfectly conjugate [2]; therefore, it has become to the first priority to control the effects of this pattern on geared system. Industries and researchers have used so many methods in order to decrease effects of fluctuation of TE [2]. Micro-geometric modification is one of the common intentional removal of material from the gear teeth flanks, which is extensively used to compen-

sate for the elastic gear and tooth deflection from the applied torque. Lin et al. [3] ascertained influences of profile modification by means of linear and parabolic teeth relief on the dynamic responses and dynamic load factors of spur gears by using computational simulation techniques. Kahraman and Blankenship [4] carried out experimental analysis on spur gear in order to check influence of different linear tip modifications on dynamic response of several pairs in different input torques.

So many researches have been done on bevel gears numerically and experimentally, particularly the straight bevel gears. Terauchi et al. [5] designed a test machine in order to investigate dynamic load of gear teeth, the torque variation and the bending vibration of straight bevel gear shafts. Oda et al. [6,7] investigated root stress, bending fatigue strength and dynamic load of straight bevel gear through experiments. They focused on the dynamic behavior of straight bevel gear in a technical report [8]. Nalluveettil and Muthuveerappan [9] produced a tooth of straight bevel gear and used finite element method to evaluate bending stress of a gear tooth, and then numerical outcomes were compared with experimental data. Gagnon et al. [10] employed linear finite strip method to compute deflection of teeth of spur and straight bevel gear. A different approach named Tredgold Approximation was developed by Elkholy et al. [11] that has divided face width of straight bevel gear to a number of artificial spur gears. Load and stress distributions have been determined on each section by using analytical equations. Results of this method have been validated with experimental measurements given by Ref. [5]. Wang et al. [12] proposed a nonlinear dynamic model of bevel gear including gears, bearings and shafts. They investigated nonlinear influences of axial, lateral and torsional stiffnesses of shaft on the vibration of the bevel gear system. Marambedu [13] developed a full finite element model to compute compliance of straight bevel gear teeth with considering load distribution, transmission error and contact stress. Bahrami et al. [14] used Tredgold approximation in order to evaluate Hertzian stress distribution on the face width of straight bevel gear.

Some theoretical investigations have been done in dynamics and vibration of bevel gears. Yinong et al. [15] carried out a nonlinear analysis on multiple degree of freedom spiral bevel gear using asymmetric mesh stiffness. Chang-Jian [16] performed nonlinear dynamic analysis of bevel gear system, including thrust bearing and journal bearing. Yassine et al. [17] presented dynamics of two-stage straight bevel gear in different conditions such as gear with the eccentricity defect and cracked tooth by means of numerical method; the dynamic behavior of the faulty gear system compared with the faultless system.

This paper investigates nonlinear dynamics of a straight bevel gear pair with three types of teeth modifications. The first model possesses teeth with pure involute profile, i.e., without tooth profile modification (TPM); the second model possesses teeth with modification acquired from minimizing static transmission error (STE) and the third model possesses teeth with modification acquired from optimizing dynamic transmission error (DTE). The governing equations of motion are nonlinear and time-varying due to backlash function and mesh stiffness, respectively. The periodically varying mesh stiffness is due to the change in the number of teeth in contact as the gears rotate. Time-varying mesh stiffness is evaluated by *HelicalPair* software [18]. *HelicalPair* is a software developed in the Center Intermech MO.RE. (Aster, High Technology Network of the Emilia Romagna Region). *HelicalPair* acts as a preprocessor and postprocessor for a finite element (FE) solver, namely MSC Marc software. An advanced toolbox of *HelicalPair* is tooth optimization by means of genetic algorithm (GA), which is utilized to improve performance of the case studies through modification on tip and root of involute profile.

2 Physical model

The tooth geometry of straight bevel gear is not uniform [19]. They vary from heel with wide thickness to toe with thin thickness; it introduces stiffness variation along the face width. The bevel gear face width has been divided to three different artificial spur gears; see Table 1 for geometrical details. Figure 1 illustrates the lumped parameter model developed to study the dynamic behavior of the bevel gears. Table 2 presents the common gear design parameters of straight bevel gears. The pinion is connected to the gear via three equivalent teeth mesh stiffness and three equivalent viscous dampers. Note that the translational degrees of freedom (DOF) for bevel gears have been limited in all directions, i.e., only rotational mobility of the shafts is allowed.

Table 1 Design parameters of the artificial equivalent spur gear pairs

Parameters	First slice	Second slice	Third slice
Number of teeth	45	45	45
Module (mm)	5.7	5.3	4.8
Pressure angle (°)	20	20	20
Face width (mm)	10	10	10
Tip diameter (mm)	273.08	252.2	231.3
Root diameter (mm)	247.08	228.2	209.3
Nominal torque (N mm)	125,000	119,000	103,000

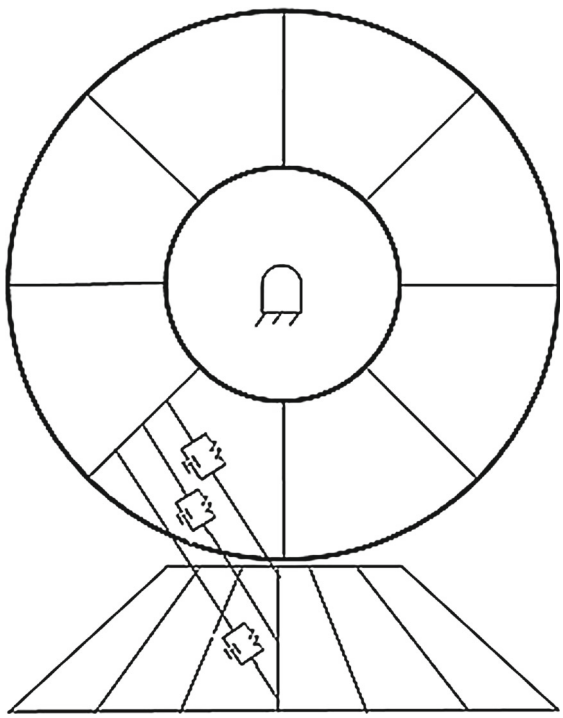

Fig. 1 Equivalent dynamic model of the straight bevel gear

The equation of motion of the system is obtained by applying Lagrange formulation [20,21] and is given by:

$$
\begin{aligned}
&I_1\ddot{\theta}_1 + c_1 r_{11}(r_{11}\dot{\theta}_1 - r_{21}\dot{\theta}_2 - \dot{e}_{pair1}) \\
&\quad + c_2 r_{12}(r_{12}\dot{\theta}_1 - r_{22}\dot{\theta}_2 - \dot{e}_{pair2}) \\
&\quad + c_3 r_{13}(r_{13}\dot{\theta}_1 - r_{23}\dot{\theta}_2 - \dot{e}_{pair3}) \\
&\quad + k_1 r_{11} f(r_{11}\theta_1 - r_{21}\theta_2 - e_{pair1}) \\
&\quad + k_2 r_{12} f(r_{12}\theta_1 - r_{22}\theta_2 - e_{pair2}) \\
&\quad + k_3 r_{13} f(r_{13}\theta_1 - r_{23}\theta_2 - e_{pair3}) = T_1
\end{aligned}
$$

Table 2 Numerical parameters of the straight bevel gear pairs

Parameters	Value
Number of teeth	32
Heel Module (mm)	6
Pressure angle (°)	20
Face width (mm)	30
Module of elasticity (MPa)	206,000
Poisson ratio	0.3
Pitch angle (°)	45
Outer cone normal backlash (mm)	0.1746
Nominal torque (N mm)	317,000

$$
\begin{aligned}
&I_2\ddot{\theta}_2 - c_1 r_{21}(r_{11}\dot{\theta}_1 - r_{21}\dot{\theta}_2 - \dot{e}_{pair1}) \\
&\quad - c_2 r_{22}(r_{12}\dot{\theta}_1 - r_{22}\dot{\theta}_2 - \dot{e}_{pair2}) \\
&\quad - c_3 r_{23}(r_{13}\dot{\theta}_1 - r_{23}\dot{\theta}_2 - \dot{e}_{pair3}) \\
&\quad - k_1 r_{21} f(r_{11}\theta_1 - r_{21}\theta_2 - e_{pair1}) \\
&\quad - k_2 r_{22} f(r_{12}\theta_1 - r_{22}\theta_2 - e_{pair2}) \\
&\quad - k_3 r_{23} f(r_{13}\theta_1 - r_{23}\theta_2 - e_{pair3}) = -T_2
\end{aligned} \tag{1}
$$

In Eq. 1, I_1 and I_2 are rotary inertia of pinion and gear, r_{11}, r_{12}, r_{13} are base radii of pinion slices, and r_{21}, r_{22}, r_{23} are base radii of gear slices, respectively. Deflections all over teeth are considered uniform, so angular displacement for slices is equal with θ_1 for driver and θ_2 for driven gear. Because of manufacturing error and/or some intentional modification on the teeth profile, a free space is produced between mating teeth, named no-load transmission error (NLTE) or $e(t)$. T_1 and T_2 are constant driver torque and breaking torque, respectively. k_j is the time-varying mesh stiffness; c_j is the damping coefficient between the meshing gear teeth of the pairs. The linear DTE along the line of action for each slices is defined as $\lambda = r_{1j}\theta_1 - r_{2j}\theta_2$ where $j = 1, 2, 3$. Hence, Eq. (1) simplified to a new rotational equation of motion is as follows:

$$I_{eq}\ddot{\lambda}_\theta + C_m(\dot{\lambda}_\theta - \dot{e}_\theta) + K_m(t) f(\lambda_\theta - e_\theta) = T_1 \tag{2a}$$

$$C_m = c_1 r_{11}^2 + c_2 r_{12}^2 + c_3 r_{13}^2 \tag{2b}$$

$$K_m = k_1 r_{11}^2 + k_2 r_{12}^2 + k_3 r_{13}^2 \tag{2c}$$

$$I_{eq} = \left(\frac{1}{I_1} + \frac{n^2}{I_2}\right)^{-1} \tag{2d}$$

$$f(\lambda_\theta - e_\theta) = \begin{cases} \lambda_\theta - e_\theta - \theta_b & \lambda_\theta - e_\theta > \theta_b \\ 0 & -\theta_b \le \lambda_\theta - e_\theta \le \theta_b \\ \lambda_\theta - e_\theta + \theta_b & \lambda_\theta - e_\theta < -\theta_b \end{cases} \tag{2e}$$

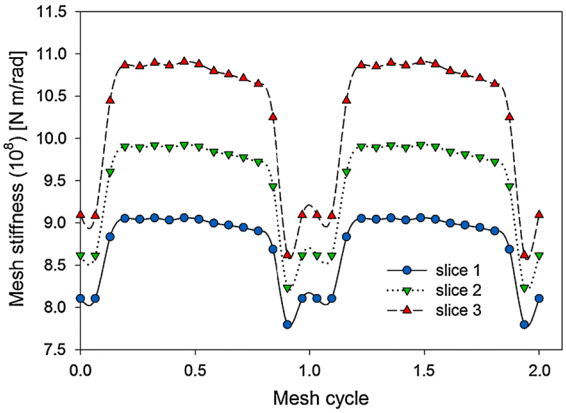

Fig. 2 Comparing torsional mesh stiffness along successive mesh cycles

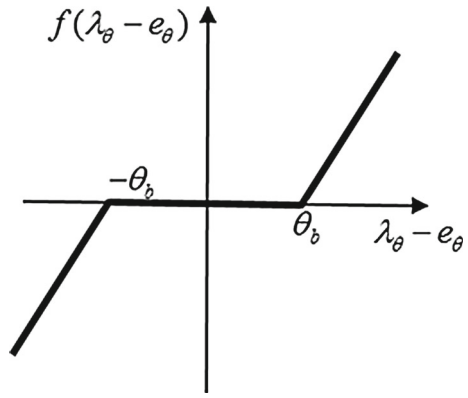

Fig. 3 Nonlinear displacement function with angular backlash

where $n = \frac{r_{2j}}{r_{1j}}$, $j = 1, 2, 3$ explains gear ratio of the gear pairs. Note that linear DTEs for pairs are not equal to each other, while angular DTEs are identical over all.

$\lambda_\theta = \theta_1 - n\theta_2$ is the angular dynamic transmission error for whole model, $e_\theta(t)$ is the time-varying circumferential NLTE of the model, and θ_b is the angular backlash. Clearly, involute profile has zero value for $e_\theta(t)$ [20]. Equation (2a) expresses dimensional nonlinear displacement function of the gear pairs. The term K_m is the equivalent of the torsional mesh stiffnesses of the gear pairs which are simultaneously time-varying and periodic by fundamental meshing frequency $\omega_m = \frac{2\pi}{60} N_1 \gamma_s$, see Fig. 2. N_1 is the teeth number of pinion, and γ_s[rpm] is the input shaft speed. Therefore, it is expanded in Fourier series:

$$K_m(t) = k_0 + \sum_{j=1}^{S} a_j \cos(j\omega_m t) + \sum_{j=1}^{S} b_j \sin(j\omega_m t) \tag{3}$$

where k_0 is the average value of torsional mesh stiffness; a_j, b_j are Fourier coefficients. Mesh stiffness and NLTE are computed from the aforementioned quasi-static program that yields angular displacement of model in $N_p = 15$, discrete rotational position over a mesh cycle. The number of samples N_p is related to the number of harmonics, $S = (N_p - 1)/2$. Figure 2 shows mesh stiffness variation for each three slices over the two successive periods. In this model, the gear meshes have single angular clearance $2\theta_b$ in spite of different normal backlash $2b_n$ along face width for other types of the gears. $f(\lambda_\theta - e_\theta)$ is the rotational displacement function which is multiplied with stiffness and produces the restoring force function in the equation of motion, see Fig. 3.

Whenever $\lambda_\theta - e_\theta$ is allocated between $+\theta_b$ and $-\theta_b$, the displacement function returns to zero, so mating teeth separate from each other and contact loss occurs due to the clearance between gear teeth [22]. For $\lambda_\theta - e_\theta > \theta_b$, the mesh is expected to be in forward contact, while in the state $\lambda_\theta - e_\theta < -\theta_b$ undesired backside contact occurs, which causes several problems in gear systems; see Ref. [20]. Equation (2a) is normalized by substituting new parameters as follows:

$$\tau = \omega_n t, \quad \omega_n = \sqrt{\frac{k_0}{I_{eq}}}, \quad \overline{e}_\theta = \frac{e_\theta}{\theta_b}, \quad \lambda' = \frac{\mathrm{d}\lambda}{\mathrm{d}\tau},$$
$$\overline{T}_g = \frac{T_1}{\theta_b I_{eq} \omega_n^2}, \quad \zeta = \frac{C_m}{2 I_{eq} \omega_n} \tag{4a}$$

$$\overline{K}_m(t) = 1 + \sum_{j=1}^{S} \frac{a_j}{I_{eq}\omega_n^2} \cos(j\omega_m t) + \sum_{j=1}^{S} \frac{b_j}{I_{eq}\omega_n^2} \sin(j\omega_m t) \tag{4b}$$

$$f(\overline{\lambda}_\theta - \overline{e}_\theta) = \begin{cases} \overline{\lambda}_\theta - \overline{e}_\theta - 1 & \overline{\lambda}_\theta - \overline{e}_\theta > 1 \\ 0 & -1 \le \overline{\lambda}_\theta - \overline{e}_\theta \le 1 \\ \overline{\lambda}_\theta - \overline{e}_\theta + 1 & \overline{\lambda}_\theta - \overline{e}_\theta < -1 \end{cases} \tag{4c}$$

$$\overline{\lambda''}_\theta + 2\zeta(\overline{\lambda'}_\theta - \overline{e'_\theta}) + \overline{K}_m(\tau) f(\overline{\lambda}_\theta - \overline{e_\theta}) = \overline{T}_g \tag{4d}$$

Equation (4d) describes a nonlinear differential equation with time-varying coefficient which excites system. A numerical integration based on fourth-order Runge–Kutta integration computes the dynamic behavior of the system. In order to validate the numerical

Table 3 Numerical parameters of the spur gear pairs of benchmark model, Ref. [23]

Parameters	Pinion	Gear
Number of teeth	50	50
Module (mm)	3	3
Pressure angle (°)	20	20
Outside diameter (mm)	156	156
Module of elasticity (MPa)	206,000	206,000
Density (kg/m^3)	7850	7850
Face width (mm)	20	20

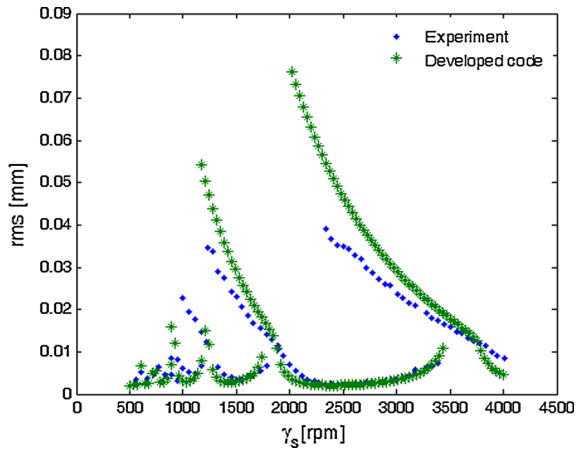

Fig. 4 Comparison between numerical simulation and experimental data from Ref. [23]

outputs of the dynamic solver, its outputs are compared with experimental data of Kahraman and Blankenship [23]. The test has been carried out on a spur gear using data of Table 3.

The gear set was tested by 340 Nm torque in the speed range between 500 and 4000 (rpm). The dynamic solver records root-mean-square (rms) of DTEs in 100 increments along the last ten steady state periods. Numerical solutions match quite well with the experimental data; see Fig. 4. Nonlinear softening behavior and jump phenomena are almost coincide with experimental data. In addition to the primary resonance at $\omega_m/\omega_n \approx 1$, two secondary resonances (super harmonics) at approximately $\omega_m/\omega_n \approx 1/2$ and $\omega_m/\omega_n \approx 1/3$ have excellent agreement with Ref. [23].

Angular rotations of each three slices along the face width are considered equal to each other. As well as static results, the dynamic responses present good agreement for all three slices; Fig. 5 illustrates this compatibility.

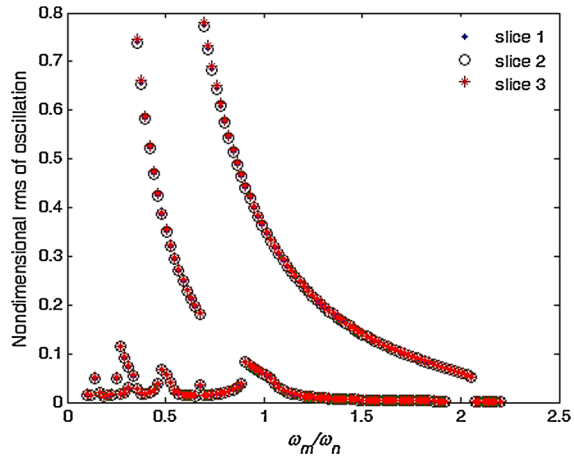

Fig. 5 Comparison of the dimensionless rms of three slices versus dimensionless excitation frequency

3 Optimized profile modification

The modification procedure employed in this study is the same as in Ref. [24] including selection, crossover and mutation with certain number of interactions on population of strings. The genetic algorithm model randomly selects first population. The best chromosome based on its highest fitness, i.e., lowest peak to peak of transmission error for static model and lowest value of dynamic transmission error for dynamic model, is thus selected. Eight parameters including four amplitudes and four diameters of modification are achieved from genetic algorithm, which identify the set of profile modification on both pinion and gear profiles. From operating pitch diameter to tip diameter and from operating pitch diameter to root diameter are allowable searching ranges for tip relief and root relief, respectively; amplitude for removal at operating pitch diameter is zero.

Several tests have been carried out to achieve an appropriate optimization for operating condition of the bevel gear pair. In this study, TPM encompasses tip and root relief method, linearly. One type of optimization is based on minimizing peak to peak of static transmission error of the gear sets under operating load, and the other type of optimization focuses on reduction in maximum dynamic transmission error. Para-

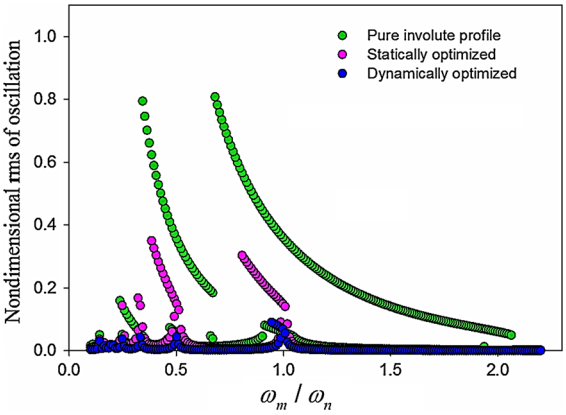

Fig. 6 Comparison of rms amplitudes for three case studies

meters of the optimized models passed to dynamic simulator in order to evaluate influence of modifications on dynamic behavior of the system. Root-mean-square (rms) is a beneficial tool to evaluate dynamic behavior in the range of pinion speed. The initial conditions for the first increment are considered as $\lambda(0) = 1.0001, \lambda'(0) = 1 \times 10^{-5}$. Consecutive increments assign initial condition from the last point of the last period. Simulation includes increasing frequency ratio (forward simulation) and decreasing frequency ratio (backward simulation). Figure 6 indicates rms amplitudes of original and modified gear pairs illustrating the nonlinear behavior of the gear sets. There is a jump down in primary resonance and super harmonics (particularly at $\omega_m/\omega_n \approx 1/2$) in backward simulation of involute profile gears. Due to modifications, the gaps decreased noticeably from 0.646 to 0.312 and 0.088 for statically optimized profile and dynamically optimized profile, respectively. Markedly, both optimizations stand out their drastic influence on gear dynamic around $\omega_m/\omega_n \approx 2$ where oscillation frequency is close to twice natural frequency (principal parametric resonance) [25]. It is well known that parametrically excited systems undergo to parametric instability gives rise to 2T respond. It is the other source of oscillation in dynamic systems, but the jumps are eliminated by applying profile modifications. It is important to compare average values of the amplitudes of the cases. Due to STE optimization and DTE optimization, the mean quantities of amplitudes are decreased 80 and 97 %, with respect to pure involute tooth profile.

4 Nonlinear dynamic behavior of straight bevel gear

Dynamic behavior of the systems can be analyzed with different beneficial tools. Bifurcation analysis shows a qualitative change in the features of a system, such as the number and type of solutions, under the variation of one or more parameters [26]; therefore, bifurcation map illustrates some specific information of nonlinear dynamic responses.

Dimensionless frequency or dimensionless rotational speed (ω_m/ω_n) is the bifurcation control parameter which varies between 0.1 and 2.2 during analyzing, continuously. There are some other applicable control parameters in geared system, see Ref. [27]. The variable control parameter domain was discretized to 300 steps. The state variables at the end of one integration step are taken as the initial values for the next step.

Dynamic behavior of involute tooth profile gear is shown in Figs. 7 and 8 for speed-up and speed-down, respectively. In backward motion, from 2.2 to 2.073 symmetric periodic solutions are achieved with excitation frequency ω_m; the periodic solution switches to period-doubling bifurcation with precisely one-half of the excitation frequency, $\omega_m/2$. Two branches emerge until the frequency ratio approach to approximately 0.6804. The rate of variation the upper branch is smooth, while the other one changes sharply.

The period-doubling bifurcation behavior is repeated for speed-up around $\omega_m/\omega_n \approx 2$ and in the short range between 0.654 and 0.676; the other frequency ratios have period-one response with asymptotic trend near super-harmonics, see Fig. 8. The time

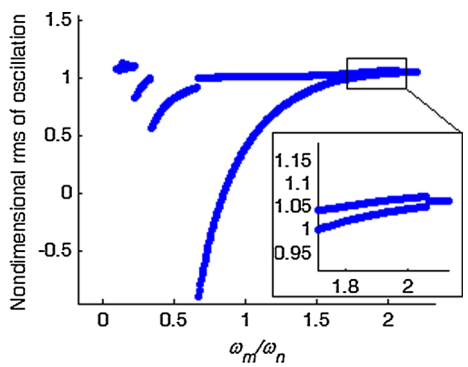

Fig. 7 Bifurcation diagram of backward motion of involute tooth profile

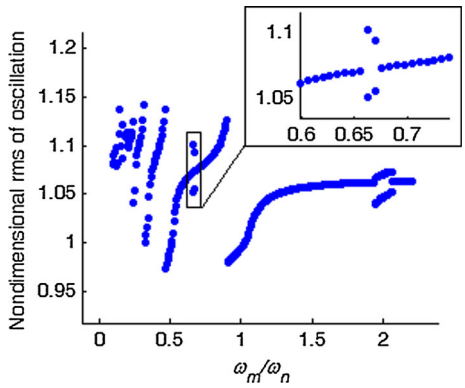

Fig. 8 Bifurcation diagram of forward motion of involute tooth profile

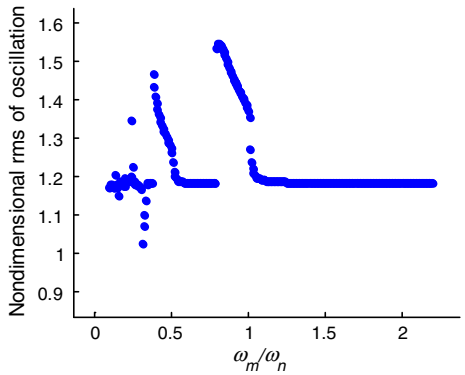

Fig. 10 Bifurcation diagram of backward simulation—statically optimized teeth

response curve, phase portrait and Poincaré map of the presented bevel gear system are illustrated for frequency ratios equal to 2.003 (case 1) and 0.6618 (case 2) in backward and forward simulations, respectively; see Fig. 9. Two separate points in Poincaré map of case 1 indicate period 2-T_m in backward motion. Green stars on the time history and phase portrait curves show starting points of the corresponding excitation period.

By employing TPM, the period-doubling bifurcation disappeared; i.e., for the excitation frequency range in that period doubling occurred, the response switched to periodic motion. Figure 10 presents bifurcation diagram of the bevel gears system with statically optimized system, and Fig. 11 presents bifurcation diagram of the bevel gears system with dynamically optimized system.

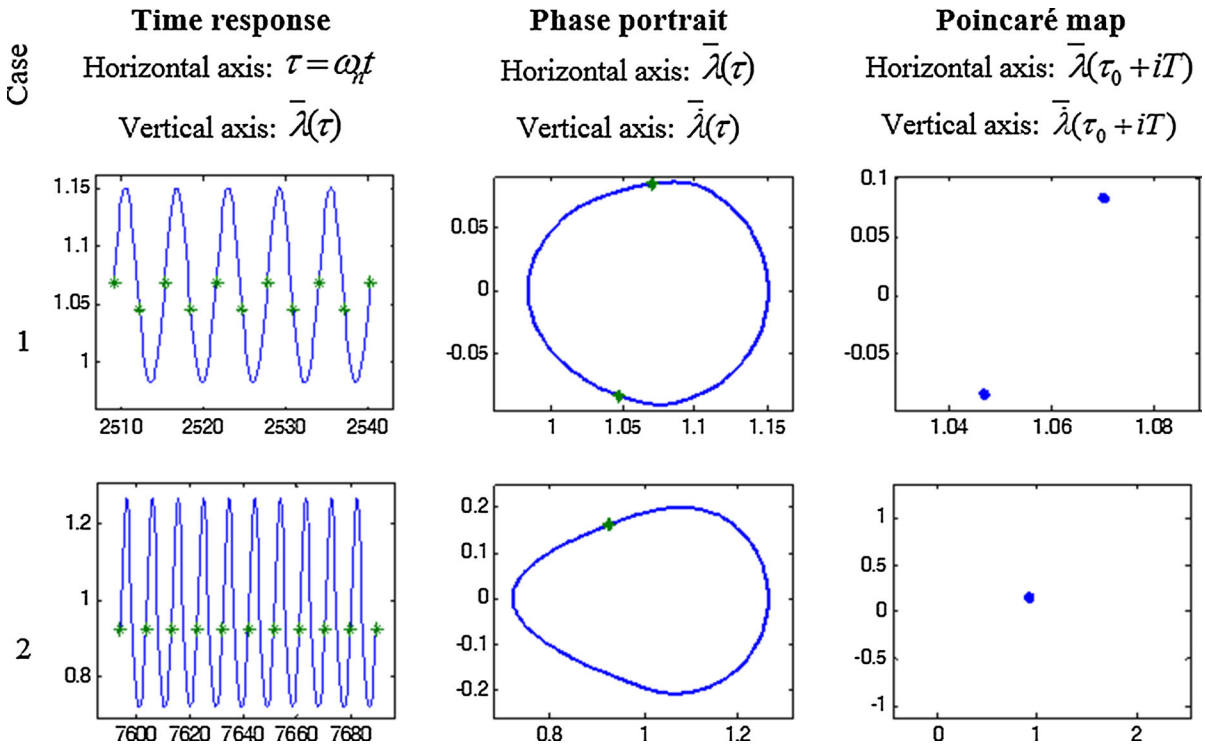

Fig. 9 Vibration attractors in 2.003 in speed-up (case 1), and 0.6618 (case 2) in speed-down motion

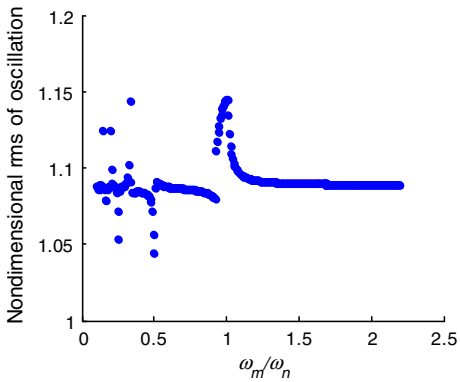

Fig. 11 Bifurcation diagram of backward simulation—dynamically optimized teeth

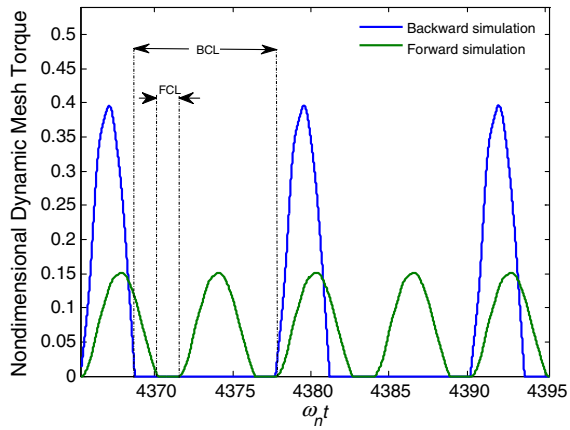

Fig. 12 Mesh Restoring Torque variation of the involute tooth profile; *BCL* backward contact loss, *FLC* forward contact loss

5 Dynamic load factor

The repetitive dynamic load provides condition to arise fatigue failure in the tooth root, pitting and scoring on the teeth surface. Reduction in gear dynamic load is one of the major concerns in the design of power transmission gears [3]. Leftward-leaning resonant response indicates softening nonlinearity due to stiffness reduction in the system as the gears lose contact at large vibrations. Dynamic mesh force (DMF) is defined as restoring force of gear mesh set [21,28]. Due to variation of pitch radius of the bevel gears tooth from heel to toe, we introduce dynamic mesh torque (DMT) instead of DMF. $\overline{\mathrm{DMT}}$ introduced as non-dimensional dynamic restoring mesh:

$$\overline{\mathrm{DMT}} = \overline{K}_m(\tau) f(\overline{\lambda}_\theta - \overline{e}_\theta) \tag{5}$$

Figure 12 illustrates DMT among successive cycles for both forward and backward simulation at frequency ratio $\omega_m/\omega_n = 1.007$ for the case of involute tooth profile. This frequency is very close to primary resonance region. In some segments of period, DMT values vanish; i.e., loss of contact. Contact loss domain in backward simulation is more than corresponding domain in forward simulation; the ratio of forward contact loss domain over a total mesh frequency period (FCL/T_{mf}) in forward simulation is about 0.23, while this ratio of backward simulation (BCL/T_{mb}) is almost 0.72; where T_{mf} and T_{mb} are periods of responses of forward and backward simulations, respectively. Besides, Fig. 6 illustrates that there is a large difference between forward and backward simulations. Note that for a wide range of the given frequencies, the backward simulation is on a period-doubling branch.

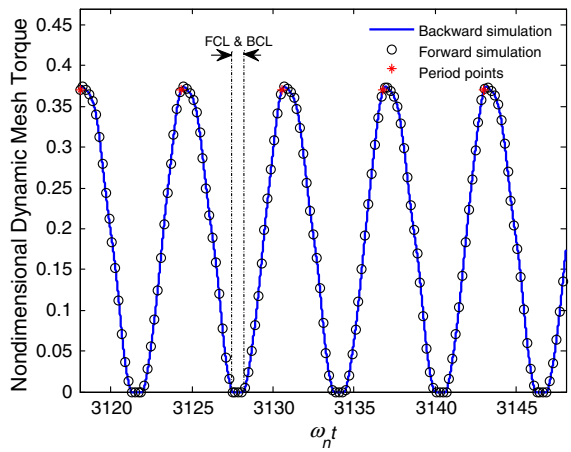

Fig. 13 Mesh restoring torque fluctuation for the statically optimized TPM, *BCL* backward contact loss, *FLC* forward contact loss

Figure 13 illustrates the influence of static optimization on the straight bevel gear mesh restoring torque at $\omega_m/\omega_n = 1.007$ in both forward and backward simulations. By augmenting TPM, duration of contact loss is reduced 92 and 51 % compared with involute tooth profile gear in backward and forward simulations, respectively; furthermore, the backward and forward simulations superimposed on each other; i.e., BCL = FCL.

Figure 14 shows DMT for the case of bevel gear with dynamically optimized TPM on the straight bevel gear mesh restoring torque at $\omega_m/\omega_n = 1.007$. Contrary to statically optimized teeth, the contact loss region is disappeared and DMT fluctuation is sensibly reduced. Therefore, TPM decreases dynamic ampli-

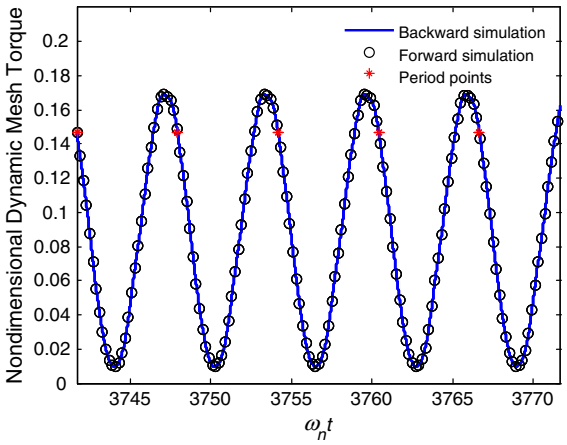

Fig. 14 Mesh restoring torque fluctuation for the dynamically optimized TPM

tude of responses and improves the force behavior of the system.

A non-dimensional parameter is introduced as dynamic mesh torque factor. It is the ratio of maximum value of the dynamic mesh torque in one complete mesh cycle of the steady state response to the maximum value of static mesh torque (SMT) during the same cycle [28], Eq. (6):

$$(\mathrm{DF})_{RT} = \frac{(\overline{\mathrm{DMT}})_{\max}}{\overline{\mathrm{SMT}}} \tag{6}$$

where $\overline{\mathrm{SMT}} = \overline{T}_g$ is the non-dimensional static mesh torque used in non-homogenous part of equation of motion, Eq. (4d).

Data in Table 4 are dynamic restoring torque factors for a specific frequency $\omega_m/\omega_n = 1.007$. The dynamic factor of the bevel gear with dynamically optimized TPM is less than one-third of corresponding value for the involute tooth profile case.

6 Discussion and conclusion

In this manuscript, the effects of tooth profile modification on the nonlinear dynamic behavior of the straight bevel gear systems are investigated. For this reason, bevel gear teeth are simplified using Tredgold method, and thus the artificial teeth are analyzed statically to evaluate mesh stiffnesses. Tooth profile modifications employed in order to optimize the dynamic response of the bevel gear by means of genetic algorithm toolbox of *HelicalPair* software. The optimal TPM is obtained

Table 4 Comparison of the dynamic torque factors for models with and without modification

Modification	$(\mathrm{DF})_{RT}$
Involute tooth profile	5.98
Statically optimized teeth	2.07
Dynamically optimized teeth	1.91

by two methods: static optimization and dynamic optimization. The statically optimized TPM is obtained by minimizing the static transmission error fluctuation, which leads to decline the average value of DTE 80 % with respect to pure involute teeth case. Besides, the dynamically optimized TPM is obtained by minimizing the rms of the DTE, which leads to decline in the average value of DTE (more than 97 %). It is worthwhile to obtain a noiseless gearbox. Both models are compared with the involute tooth profile model. There are some regions in involute tooth profile model in that rms of responses jump up or down depend on forward or backward motion. The maximum amplitude of jumps is reduced noticeably for statically and dynamically optimized tooth profiles, nearly 52 and 86 % respectively.

It is observed that in optimized models, the period-doubling bifurcation regions are disappeared and their leftward-leaning behavior (softening nonlinearity) decreased. Furthermore, dynamic mesh torque factor $(\mathrm{DF})_{RT}$ in dynamically optimized model has better behavior than statically optimized model.

Acknowledgments The authors would like to thank the Lab SIMECH/INTERMECH MO.RE. (HIMECH District, Emilia Romagna Region) particularly Prof. Francesco Pellicano and Dr. Marco Barbieri for providing FEM code and their guidance during the research.

References

1. Smith, J.: Gear Noise and Vibration. Marcel Dekker Inc., New York (1999)
2. Åkerblom, M., Pärssinen, M.: A Study of Gear Noise and Vibration. TRITA-MMK 2002:8/ISSN 1400-1179/ISRN/KTH/MMK/R-02/8-SE, Stockholm (2002)
3. Lin, H.H., Oswald, F.B., Townsend, D.P.: Dynamic loading of spur gears with linear or parabolic tooth profile modifications. Mech. Mach. Theory **29**(8), 1115–1129 (1994)
4. Kahraman, A., Blankenship, G.W.: Effect of involute tip relief on dynamic response of spur gear pairs. J. Mech. Des. **121**(2), 313–315 (1999)
5. Terauchi, Y., Miyao, Y., Fujii, M.: Dynamic behavior of straight bevel gear—1. Dynamic load, torque variation and

bending vibration of gears shafts. Bull. JSME **23**, 126–131 (1980)
6. Oda, S., Koide, T., Okamura, Y.: Dynamic behavior of straight bevel gear of Gleason type. Bull. JSME **26**, 216–220 (1983)
7. Oda, S., Koide, T., Okamura, Y.: Study on bending fatique of straigth bevel gears. Bull. JSME **25**, 1173–1179 (1982)
8. Oda, S., Takao, K., Higuchi, K.: Study on bending fatique of straigth bevel gears. Bull. JSME **26**, 140–145 (1983)
9. Nalluveettil, S.J., Muthuveerappan, G.: Finite element modelling and analysis of a straight bevel gear tooth. Comput. Struct. **48**(4), 739–744 (1993)
10. Gagnon, P., Gosselin, C., Cloutier, L.: Analysis of spur and straight bevel gear teeth deflection by the finite strip method. J. Mech. Des. **119**, 421–426 (1997)
11. Elkholy, A., Elsharkawy, A., Yigit, A.S.: Effect of meshing tooth stiffness and manufacturing error on the analysis of straight bevel gears. J. Struct. Mech. **26**(1), 41–61 (1998)
12. Wang, Y., Cheung, H.M.E., Zhang, W.J.: 3D dynamic modelling of spatial geared systems. Nonlinear Dyn. **26**(4), 371–391 (2001)
13. Marambedu, K.R.: Development of a procedure for the analysis of load distribution, stresses and transmission error of straight bevel gears. The Ohio State University (2009)
14. Bahramighahnavieh, A., Mosaddegh, P., Akbarzadeh, S.: Investigation of the Hertzian stress distribution on the surface of the straight bevel gear. Appl. Mech. Mater. **307**, 304–307 (2013)
15. Yinong, L., Guiyan, L., Ling, Z.: Influence of asymmetric mesh stiffness on dynamics of spiral bevel gear transmission system. Math. Prob. Eng. (2010). doi:10.1155/2010/124148
16. Chang-Jian, C.-W.: Nonlinear dynamic analysis for bevel-gear system under nonlinear suspension-bifurcation and chaos. Appl. Math. Model. **35**, 3225–3237 (2011)
17. Yassine, D., Hammami, A., Walha, L., Haddar, M.: Effects of gear mesh fluctuation and defaults on the dynamic behavior of two-stage straight bevel system. Mech. Mach. Theory **82**, 71–86 (2014)
18. Barbieri, M., Zippo, A., Pellicano, F.: Adaptive grid-size finite element modeling of helical gear pairs. Mech. Mach. Theory **82**, 17–32 (2014)
19. Maitra, G.: Handbook of Gear Design. Tata McGraw-Hill Education, New York (1994)
20. Bonori, G.: Static and dynamic modeling of gear transmission error. Ph.D. Thesis, University of Modena and Reggio Emilia (2006)
21. Kahraman, A., Lim, J., Ding, H.: A dynamic model of a spur gear pair with friction. In: Proceedings of the 12th IFToMM World Congress (2007)
22. Liu, G., Parker, R.G.: Nonlinear dynamics of idler gear systems. Nonlinear Dyn. **53**(4), 345–367 (2008)
23. Kahraman, A., Blankenship, G.: Experiments on nonlinear dynamic behaviour of an oscillator with clearance and periodically time-varying parameters. J. Appl. Mech. **64**, 217–226 (1997)
24. Bonori, G., Barbieri, M., Pellicano, F.: Optimum profile modifications of spur gears by means of genetic algorithms. J. Sound Vib. **313**(3), 603–616 (2008)
25. Nayfeh, A.H., Mook, D.T.: Nonlinear Oscillations. Wiley, New York (1979)
26. Nayfeh, A.H., Balachandran, B.: Applied Nonlinear Dynamics: Analytical, Computational and Experimental Methods. Wiley, New York (2004)
27. Kahraman, A.: On the response of a preloaded mechanical oscillator with a clearance: period-doubling and chaos. Nonlinear Dyn. **3**(3), 183–198 (1992)
28. Tamminana, V.K., Kahraman, A.: A study of the relationship between the dynamic factors and the dynamic transmission error of spur gear pairs. J. Mech. Des. **129**, 75–83 (2007)